

# Geophysical Research Letters<sup>®</sup>

## RESEARCH LETTER

10.1029/2022GL099727

### Key Points:

- Convection-permitting model reproduces the observed super Clausius-Clapeyron scaling for hourly extreme precipitation over South Korea
- Precipitation type analysis using convective available potential energy reveals the important role of convection in the scaling
- The role of convection becomes dominant in the high-emission scenario, resulting in unprecedented extreme rainfall events in late summer

### Supporting Information:

Supporting Information may be found in the online version of this article.

### Correspondence to:

S.-K. Min,  
[skmin@postech.ac.kr](mailto:skmin@postech.ac.kr)

### Citation:

Lee, D., Min, S.-K., Park, I.-H., Ahn, J.-B., Cha, D.-H., Chang, E.-C., & Byun, Y.-H. (2022). Enhanced role of convection in future hourly rainfall extremes over South Korea. *Geophysical Research Letters*, 49, e2022GL099727. <https://doi.org/10.1029/2022GL099727>

Received 24 MAY 2022

Accepted 25 OCT 2022

## Enhanced Role of Convection in Future Hourly Rainfall Extremes Over South Korea

Donghyun Lee<sup>1,2</sup>, Seung-Ki Min<sup>2</sup> , In-Hong Park<sup>3</sup>, Joong-Bae Ahn<sup>4</sup> , Dong-Hyun Cha<sup>5</sup> , Eun-Chul Chang<sup>6</sup> , and Young-Hwa Byun<sup>7</sup>

<sup>1</sup>Environmental Change Institute, School of Geography and the Environment, University of Oxford, Oxford, UK, <sup>2</sup>Division of Environmental Science and Engineering, Pohang University of Science and Technology, Pohang, South Korea, <sup>3</sup>Department of Marine Sciences and Convergence Technology, Hanyang University, Ansan, South Korea, <sup>4</sup>Department of Atmospheric Sciences, Pusan National University, Busan, South Korea, <sup>5</sup>Department of Urban and Environmental Engineering, Ulsan National Institute of Science and Technology, Ulsan, South Korea, <sup>6</sup>Department of Atmospheric Sciences, Kongju National University, Gongju, South Korea, <sup>7</sup>Climate Change Research Team, National Institute of Meteorological Sciences, Seogwipo, South Korea

**Abstract** A convection-permitting regional climate model (CPRCM) with 2.5 km resolution has been simulated over South Korea for current and future conditions, and the role of convection in the scaling of hourly extreme precipitation (EP) with temperature is examined. It is found that the CPRCM can reproduce the observed super Clausius-Clapeyron (C-C) scaling for hourly EP. Precipitation type estimated based on the convective available potential energy reveals the important role of convection in the super C-C scaling. Fraction of convective rainfall events increases rapidly with temperature, and the contribution of convection becomes dominant in future simulations under high-emission scenarios. In the late 21st century, as temperature ranges shift to warmer conditions, unprecedented hourly extreme rainfall events are projected to occur particularly during the late summer season. Future changes in hourly extreme events are found to be affected much by boundary conditions from different global climate models.

**Plain Language Summary** The role of convection in the scaling of hourly extreme precipitation (EP) with temperature is examined using convection-permitting regional climate model simulations. The convection-permitting model has been simulated over South Korea with 2.5 km resolution for current and future conditions. The model is found to capture the observed super Clausius-Clapeyron (C-C) scaling, which is underestimated by a low resolution simulation based on convective parameterization. When analyzing contributions of convective versus non-convective type events based on convective available potential energy, convective events are found to be more important in shaping the super C-C scaling. As the proportion of convective precipitation increases rapidly with warming, the role of convection in the scaling becomes dominant. Future projections under high emission scenarios indicate the occurrence of unprecedented hourly EP events during the late summer season. It is also found that global climate model boundary conditions affect the EP-temperature scaling by providing different background warming rates.

## 1. Introduction

An increasing number of studies have examined the dependence of sub-daily extreme rainfall intensity on the surface air temperature, so-called extreme precipitation-temperature (EP-T) scaling as reviewed by Fowler et al. (2021). The scaling rates identified in the observations were found to be larger than the theoretical limit of the Clausius-Clapeyron (C-C) relation, suggesting disproportionate intensification of sub-daily precipitation extremes in a warmer condition. Several observational studies confirmed this short-term EP-T relationship over various regions: Europe (Berg & Haerter, 2013; Blenkinsop et al., 2015; Busuioc et al., 2017; Drobinski et al., 2016; Lenderink & van Meijgaard, 2010), North America (Ivancic & Shaw, 2016; Lepore et al., 2015; Panthou et al., 2014), Australia (Hardwick Jones et al., 2010; Wasko & Sharma, 2014), and Asia (Fujibe, 2013; Hatsuzuka et al., 2021; Lenderink et al., 2011; Park & Min, 2017; Utsumi et al., 2011; Wang et al., 2018; Xiao et al., 2016). These sub-daily rainfall scaling rates were generally higher than those for daily rainfall, confirming that hydrological extremes at shorter timescales are more sensitive to surface warming levels (Drobinski et al., 2016; Park & Min, 2017; Utsumi et al., 2011; Wang et al., 2018).

The convective process has been suggested as an important dynamic mechanism for the super C-C scaling by enhancing the EP intensity beyond the thermodynamic threshold (Fowler et al., 2021). To classify precipitation types, some studies used the observations of cloud types: stratiform versus convective (e.g., Berg et al., 2013; Lenderink et al., 2011; Park & Min, 2017), and others applied convection available potential energy (CAPE) or duration-based thresholds (Barbero et al., 2019; Hatsuzuka et al., 2021; Maranan et al., 2019; Panthou et al., 2014; Visser et al., 2020). Regardless of different methods, those observational analyses consistently found the enhanced role of convection in extreme rain events at warmer atmospheric conditions.

Compared to the observed scaling, most Global Climate Models (GCMs) and traditionally used large-scale Regional Climate Models (RCMs) underperform the sub-daily extreme rainfall intensity, majorly due to their low resolutions to resolve the convective process. Convective parameterization applied in GCMs and RCMs imprecisely calculates convection in a subgrid scale with missing processes associated with several small-scale interactions (Rio et al., 2019). This induces rainfall more frequently, leading to weaker short-term rainfall (Drobinski et al., 2016; Kendon et al., 2019; Lenderink & van Meijgaard, 2010; Oh & Sushama, 2020; Suhas & Zhang, 2015; Wehner et al., 2021). By comparing two RCM simulations in identical resolutions but with different parameter settings, some studies showed that the proper setting of physics is also important to simulate weather systems responsible for sub-daily extreme rainfall events (Ahrens & Leps, 2021; Fosser et al., 2015; Sugimoto & Takahashi, 2016).

To overcome the limitations of GCMs and RCMs, high resolution convection-permitting regional climate model (CPRCM) has been utilized, which directly simulates the convective processes. Many CPRCM studies were conducted over Europe, North America, and East Asia (e.g., Belusic et al., 2020; Kendon et al., 2017; Li et al., 2020; Lucas-Picher et al., 2021; Murata, Sasaki, Kawase, & Nosaka, 2017; Prein et al., 2015; Qing & Wang, 2021). They showed the overall improved simulation skills for hourly precipitation characteristics compared to corresponding RCMs. Several studies also used CPRCM for future projections (Ban et al., 2015; Fosser et al., 2020; Helsen et al., 2020; Murata, Sasaki, Kawase, & Nosaka, 2017; Pichelli et al., 2021; Prein et al., 2017; Purr et al., 2021; Rasmussen et al., 2020). Results indicate large inter-model differences in future changes in the EP, depending on the regions and/or boundary conditions implemented (Fosser et al., 2020; Helsen et al., 2020; Murata, Sasaki, Kawase, Nosaka, et al., 2017; Pichelli et al., 2021; Prein et al., 2017). However, the role of convection in the future changes in EP-T scaling remains unexplored as most of CPRCM studies simply assumed that intense rainfall will dominate at warmer temperatures. Purr et al. (2021) is the only study that compared high and low CAPE conditions and found the enhanced role of convection in the scaling over Germany. East Asian CPRCM studies focused on assessing EP evaluations and projections (Li et al., 2020; Murata, Sasaki, Kawase, & Nosaka, 2017; Murata, Sasaki, Kawase, Nosaka, et al., 2017; Qing & Wang, 2021) and the EP-T scaling and associated mechanisms have not been analyzed even for the current climate. For South Korea, an observational study revealed that convection plays an important role in inducing super C-C scaling in hourly extreme rainfall (Park & Min, 2017), but there has been no CPRCM experiment to confirm the observational evidence and further assess future changes in the EP-T scaling.

In this study, CPRCM simulations are conducted over South Korea for current and future conditions. Using current simulations, CPRCM performance at simulating hourly EP and its scaling with temperature is evaluated in comparison with observations and low resolution RCM runs. CPRCM-simulated future changes in hourly extreme rainfall are assessed, focusing on warming-induced changes in scaling patterns and the associated occurrence of unprecedented wet events. For both present and future simulations, the role of convection is explored by considering convective and non-convective events selected based on CAPE thresholds. Further, results from two different GCM boundary conditions are compared to assess related uncertainties.

## 2. Models and Methods

### 2.1. Observations

Daily mean surface temperature, relative humidity, pressure, and hourly precipitation were obtained from the Korea Meteorological Administration (KMA) for 2001–2005 (the period of CPRCM current simulations, see below). April to October is considered to focus on warm season rainfall following Park and Min (2017). Some stations were excluded prior to analysis: Yangpyeoung and Icheon which are located too close from neighboring stations, and Baengnyeongdo, Ulleungdo, and four stations in Jeju Island, which lie outside of the analysis

domain. As a result, 65 stations were used (Figure S1 in Supporting Information S1), which have full records during the analysis period (7 stations have less than 0.04% missing values in relative humidity only). Since the selected stations have similar temperature ranges (Figure S2 in Supporting Information S1), all data from 65 stations were aggregated into a pooled set for the scaling calculation as done in Park and Min (2017). We have calculated the CAPE and CIN (convective inhibition) values using vertical profiles of temperature and water vapor mixing ratio from the European Center for Medium-Range Weather Forecasts (ECMWF) reanalysis version 5 (ERA5; Hersbach et al., 2020), which has around 30 km resolution.

## 2.2. Model Simulations

The Consortium for Small-scale Modeling (COSMO) model in CLimate Mode (COSMO-CLM, hereinafter CCLM) was used, which is a non-hydrostatic climate model designed to perform climate simulations from meso- $\beta$  to meso- $\gamma$  scale (Rockel et al., 2008; Steger & Bucchignani, 2020). Many studies used CCLM for RCM experiments (e.g., Dobler & Ahrens, 2010; Huang et al., 2015; Li et al., 2016; Sørland et al., 2021; Wang et al., 2013) and CPRCM experiments (e.g., Ban et al., 2014, 2015; Brisson et al., 2016; Fosser et al., 2015; Helsen et al., 2020; Purr et al., 2021; Raffa et al., 2021). Here, we used CCLM to perform both RCM (25 km resolution) and CPRCM (2.5 km) experiments. The associated model configurations are summarized in Table S1 in Supporting Information S1. The most important difference between RCM and CPRCM experiments is whether to use convective parameterization or not although the horizontal resolution difference can affect the precipitation-temperature scaling (e.g., Qiu & Im, 2021).

We carried out historical (2001–2005) and future (2091–2095) CPRCM simulations over South Korea (Figure S1 in Supporting Information S1). A double-nesting strategy was applied based on two boundary GCM forcings from MPI-ESM-LR (r11i1p1, referred to as MPI) and UKESM1-0-LL (r15i1p1f2, referred to as UKE). Two GCMs (single member from each GCM as indicated) are selected in accord with the CORDEX East Asia Phase II experiments (cf. Juzbašić et al., 2022). First, we dynamically downscaled coarse resolution GCM outputs (at  $\sim 200$  and  $\sim 250$  km resolutions for MPI and UKE, respectively) into 25 km resolution for the CORDEX-East Asia Phase II domain using RCM configuration. The RCM outputs were then downscaled into 2.5 km resolution for South Korea domain using CPRCM configuration. For future projections, high emission scenarios of RCP8.5 and SSP5-8.5 were considered for MPI and UKE, respectively. UKE exhibits stronger warming in the late 21st century than MPI, in line with its higher climate sensitivity (Meehl et al., 2020), to which stronger forcing in RCP8.5 than SSP5-8.5 might have contributed in part (O'Neill et al., 2016). We analyzed outputs from 65 grid boxes of CCLM where observation stations are located.

## 2.3. Extreme Precipitation Scaling

Dew point temperature (Td) is used to explore relations between hourly EP intensity and surface temperature, which helps to avoid negative scaling at higher temperature due to the reduced moisture availability (Kendon et al., 2019; Lenderink et al., 2017; Purr et al., 2021; Roderick et al., 2020). To estimate the slope of EP-Td scaling, we use an equal-temperature distance bin method (Lenderink et al., 2011). First, hourly wet events (precipitation  $\geq 0.1$  mm/hr) are selected from the pooled data and then grouped according to daily mean Td values in a 1°C interval. Extreme hourly precipitation is then defined as 99th percentile of hourly precipitation in each Td bin of a 2°C width. Finally, a bootstrapping method is used to estimate 90% confidence intervals of percentile values using half of the original sample following previous studies (Berg et al., 2013; Lenderink et al., 2017; Park & Min, 2017; Prein et al., 2017). Note that different Td ranges are applied between observations and model simulations according to corresponding hourly precipitation sample distributions (Figure S2 in Supporting Information S1). At least 80% out of the total grids are required to have more than 50 wet samples for each Td bin.

## 2.4. Precipitation Type Classification

The convective and non-convective types of precipitation are classified based on CAPE values following the method of Purr et al. (2021). CAPE represents the static instability that determines the severity of rising motion of air-parcel, that is, convection. Since the temporal evolution of CAPE and CIN is not necessarily in accord with the timing of extreme rain events (Loriaux et al., 2016; Maranan et al., 2019; Suhas & Zhang, 2015), we used the daily maximum CAPE values to represent the maximum atmospheric instability conditional to the daily mean

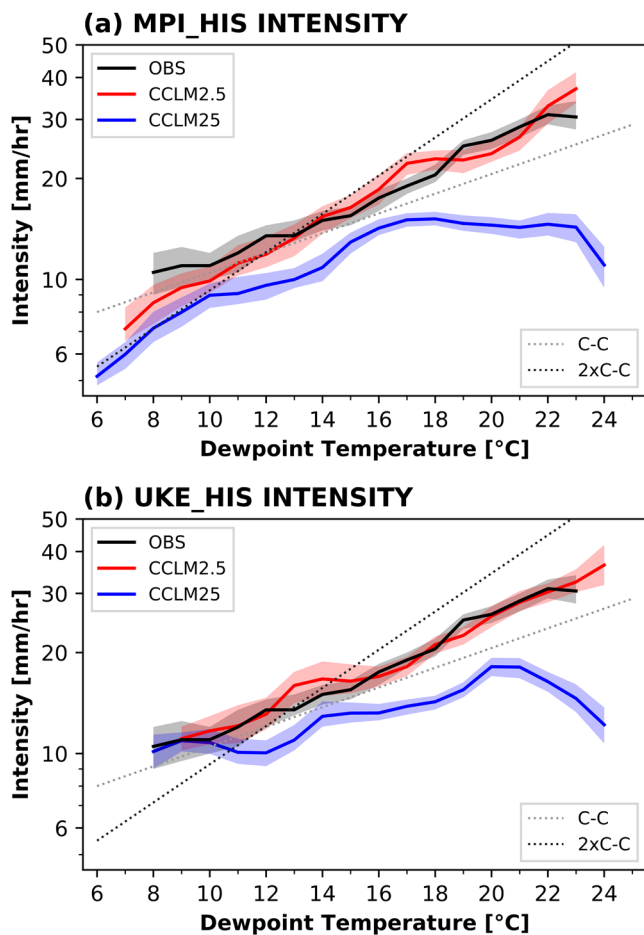


**Figure 1.** Extreme precipitation (EP) intensity (99th percentile of hourly precipitation) distributions for daily mean surface dew point temperature (Td) in CCLM simulations forced by (a) MPI-ESM-LR (MPI) and (b) UKESM1-0-LL (UKE) boundary conditions. For each, convection-permitting regional climate model (CCLM2.5, red) and RCM (CCLM25, blue) results are compared with those from observations (OBS, black). Dotted gray and black lines represent Clausius-Clapeyron (C-C) and 2x C-C scaling rates, respectively. Shaded ranges indicate 90% uncertainty diagnosed by bootstrapping methods. Note that the ordinate is scaled logarithmically.

Section 2.4). Figure 2 compares distributions of EP intensities estimated for convective type (H-CAPE) versus non-convective type (L-CAPE) cases together with a fraction of convective type events to the total EP events. Observations show that H-CAPE cases have larger EP intensities than L-CAPE cases throughout Td ranges (Figure 2a). The observed fraction of convective type gradually increases as Td increases (Figure 2d), from less than 0.2 at 8°C, 0.5 around 16°C, to near 1 above 20°C, generally consistent with the previous finding based on cloud type observations (Park & Min, 2017). Accordingly, the total precipitation scaling curve follows L-CAPE results at lower Tds and shifts onto H-CAPE results at higher Tds (Figure 1), resulting in a super C-C scaling, in line with the previous studies (Berg et al., 2013; Park & Min, 2017; Purr et al., 2021).

CPRCM simulations reproduce the greater EP intensities in H-CAPE and the dominance of convective type in higher Td ranges, with good agreement between two GCM boundary forcings (Figures 2b, 2c, 2e and 2f). In contrast, RCM simulations underestimate hourly EP intensity at higher Tds, more strongly in H-CAPE (Figures 2b and 2c). This explains RCMs' overall underestimation of EP intensity (Figure 1). Although some differences between RCM and OBS remain noticeable in 10°C–16°C ranges, RCMs can capture the observed increase in convective fraction as warming (Figures 2e and 2f). This suggests that high CAPE values in RCMs

Td bins. Note that the sign of CIN is reversed here to indicate the inhibition energy threshold for a parcel to reach the level of free convection (Maranan et al., 2019; Suhas & Zhang, 2015). We used 200 J/kg as a threshold for dividing wet samples into convective ( $\geq 200$  J/kg) or non-convective ( $< 200$  J/kg) precipitation events. When using different thresholds like 300 and 400 J/kg, main results remain unaffected (not shown). We obtained EP intensity and rainfall type fraction for high CAPE cases (H-CAPE) and compared the results with those for low CAPE (L-CAPE). Note that EP intensity for H-CAPE and L-CAPE was recomputed using corresponding subsamples to obtain the individual scaling for convective and non-convective precipitation types. CAPE and CIN were calculated from the nearest grid point of each station, and results remain unchanged when using linearly interpolated values (not shown).

### 3. Results

#### 3.1. Historical Simulations

Performances of CPRCM simulations for EP scaling are evaluated in view of observations and RCMs (Figure 1). Observations show that hourly EP (99th percentile) ranges from 10.5 to 30.5 mm/hr. The observed EP-Td scaling slopes show near C-C relation in lower Tds (7.1%/°C estimated from 8°C to 18°C) but become steeper in higher Tds (9.4%/°C estimated from 13°C to 23°C). This is largely consistent with the finding of Park and Min (2017) who used 26 stations and long-term datasets. CPRCM simulations reproduce the observed precipitation intensity range well in both GCM boundary conditions (CPRCM\_MPI: 7.1–37.0 mm/hr and CPRCM\_UKE: 11.1–36.5 mm/hr) while RCM simulations underestimate hourly extreme intensities with maxima less than 20 mm/hr. The EP-Td scaling ratio in observations (measured as a linear regression slope for a given Td range) is about 8.3%/°C, which is reasonably captured by CPRCMs (CPRCM\_MPI: 10.1%/°C and CPRCM\_UKE: 8.2%/°C). In contrast, RCMs exhibit underestimation with much weaker slopes than the C-C rate (RCM\_MPI: 5.2%/°C and RCM\_UKE: 3.1%/°C). The underestimated EP-Td scaling in RCM is due to weaker EP intensities in high Td ranges. Scaling rate differences between CPRCM and RCM become larger as Td increases, clearly indicating the improved performances of CPRCM at simulating hourly rainfall extremes in warmer conditions.

To examine the role of convection in hourly EP intensity, wet events are classified into convective or non-convective types based on CAPE values (see

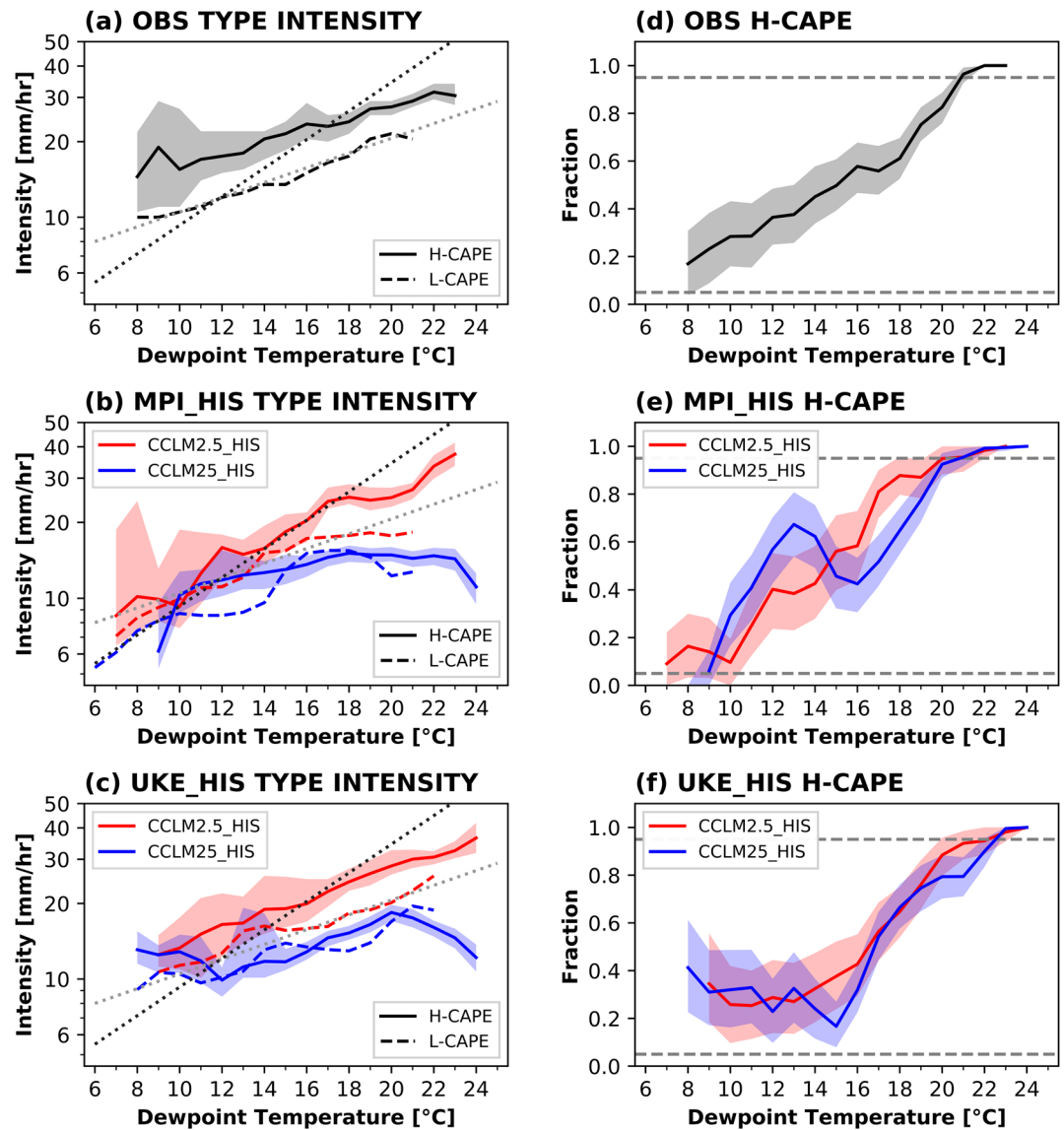


**Figure 2.** Extreme precipitation (EP) intensity distributions for dew point temperature ( $T_d$ ) from (a) observations, (b, c) CCLM simulations (CPRCM: CCLM2.5 and RCM: CCLM25) forced by MPI and UKE, respectively, computed using convective (H-CAPE, solid) and non-convective (L-CAPE, dashed) events. A logarithmical scale is applied to the ordinate. (d–f) observed and simulated distribution of the fraction of H-CAPE events to all extreme precipitation (EP) events for  $T_d$ . To exclude uncertain EP with small number of high convection available potential energy (H-CAPE) or low convection available potential energy (L-CAPE) events, we only present the EP intensity in (a–c) having number of H-CAPE or L-CAPE events larger than three for each  $T_d$ , which is equivalent to about 5% fraction of all EP events (gray dashed lines in (e) and (f)).

simulated with convective parametrization may be insufficient to derive strong convection-related hourly EP. In case of non-convective type (Figures 2b and 2c, dashed lines), EP intensities in RCM simulations show smaller differences from the CPRCM results, which indicate comparable performances of RCMs to CPRCMs in terms of large-scale precipitation extremes.

Causes of the scaling differences between CPRCMs and RCMs are further examined by comparing distributions of vertical motion, low-level moisture, and CIN under  $T_d$  ranges (Figure S3 in Supporting Information S1). It is clearly seen that RCMs simulate weaker upward motions than CPRCMs even when they have comparable strengths of CAPE and specific humidity at 850 hPa. Low-level specific humidity increases as  $T_d$  following the C-C rate until 18°C, but the increasing rate becomes weaker than moisture availability in higher  $T_d$ s. This would decrease relative humidity, leading to higher levels of condensation (LCL) and free convection (LFC). This in



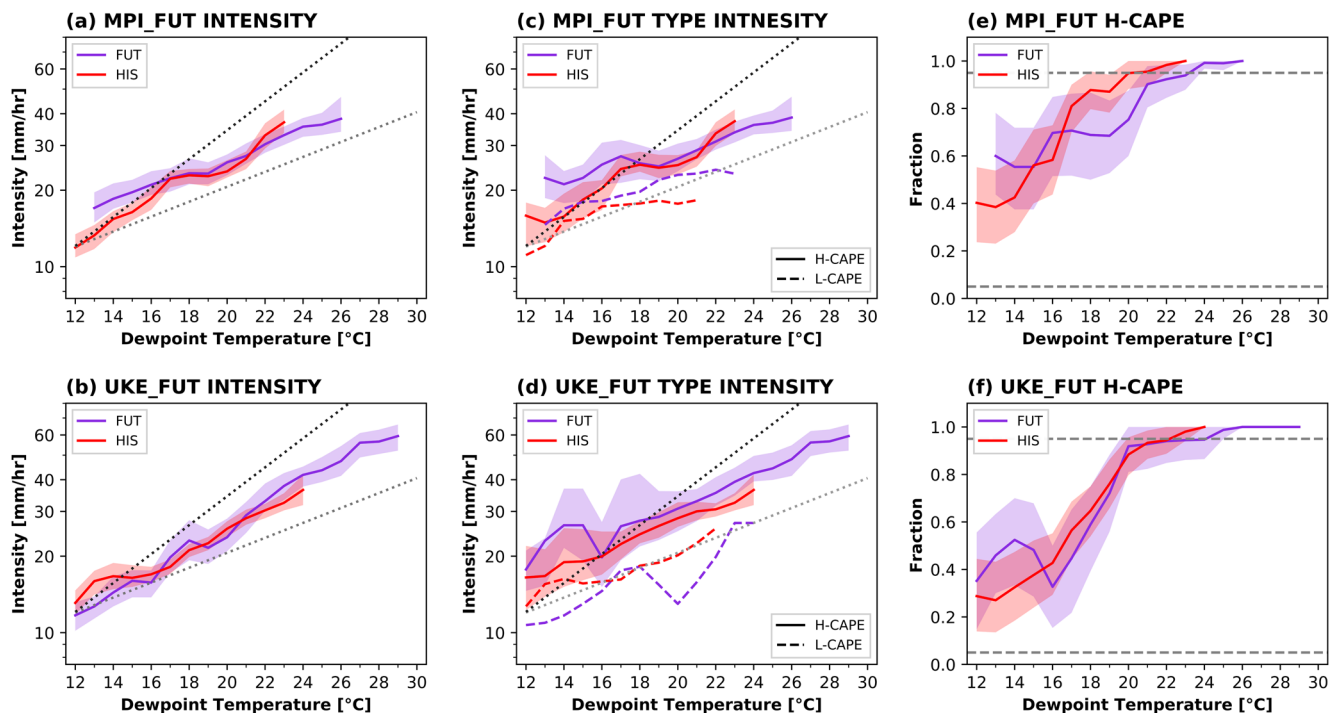


**Figure 3.** Distribution of (a, b) extreme precipitation (EP) intensity, (c, d) EP intensity in high convection available potential energy (H-CAPE) and low convection available potential energy (L-CAPE) events, and (e, f) fraction of H-CAPE to total EP events for dew point temperature from CPRCM (CCLM2.5) future simulations (FUT) forced by MPI (upper) and UKE (lower) boundary conditions. Results from corresponding historical simulations are shown together for comparison.

turn increases the amount of negative buoyancy energy CIN (Chen et al., 2020), suppressing upward motion and thereby helping to generate strong convection. Smaller CIN values in RCMs suggest that these dynamic processes are not simulated realistically. These results are in accord with Prein et al. (2021) who found differences in vertical motions between RCMs (plume-like rising column of air) and CPRCMs (thermal-like rising bubbles of air).

### 3.2. Future Projections

The impacts of future global warming on the EP-Td scaling are investigated using CPRCMs, which can capture the observed scaling rate reasonably as assessed above. When compared with historical simulations, CPRCM projections are characterized by extended Td ranges into warmer conditions (Figures 3a and 3b). CPRCM\_MPI shows an extension from 23°C to 26°C by 3°C while CPRCM\_UKE has a larger extension of 5°C from 24°C to 29°C, indicating the important influences of GCM boundary conditions on local Td distributions. As Td ranges are extended, EP intensity increases in the future. When comparing scaling slopes in H-CAPE and L-CAPE with the total case (Figures 3c and 3d), it can be seen that the total EP intensities tend to follow L-CAPE lines in cold Tds below 16°C and then make transitions to H-CAPE lines in warmer Tds above 18°C, as the convective fraction becomes larger than the non-convective fraction. The proportion of convective events remains dominant (>0.9) for the extended warm Tds above 21°C, indicating the critical role of convection in determining future hourly EP intensities. Atmospheric instability (CAPE), negative buoyant energy (CIN), thermodynamic (specific humidity), and dynamic (vertical motion) factors also show gradual increases in the extended Td bins, stretching out corresponding historical results (Figure S4 in Supporting Information S1).

Future slopes in EP-Td scaling exhibit some dependency on GCM boundary conditions such that the slope of CPRCM\_MPI becomes weaker (about 6.5%/°C) whereas the scaling remains similar in CPRCM\_UKE (10.6%/°C, Figures 3a and 3b). Different changes in the EP-Td scaling between two GCM boundary conditions can be linked to different change patterns in the convective fraction in the two models (Figures 3e and 3f). Compared to the historical values, CPRCM\_MPI shows an increase in convective fraction (>0.5) in cold Tds from 13 to 17°C and a decrease in warm Tds above 17°C (Figure 3e). This contrasting pattern seems to contribute to the weakened EP-Td slope of H-CAPE in the future relative to the historical one (Figure 3c). On the contrary, CPRCM\_UKE

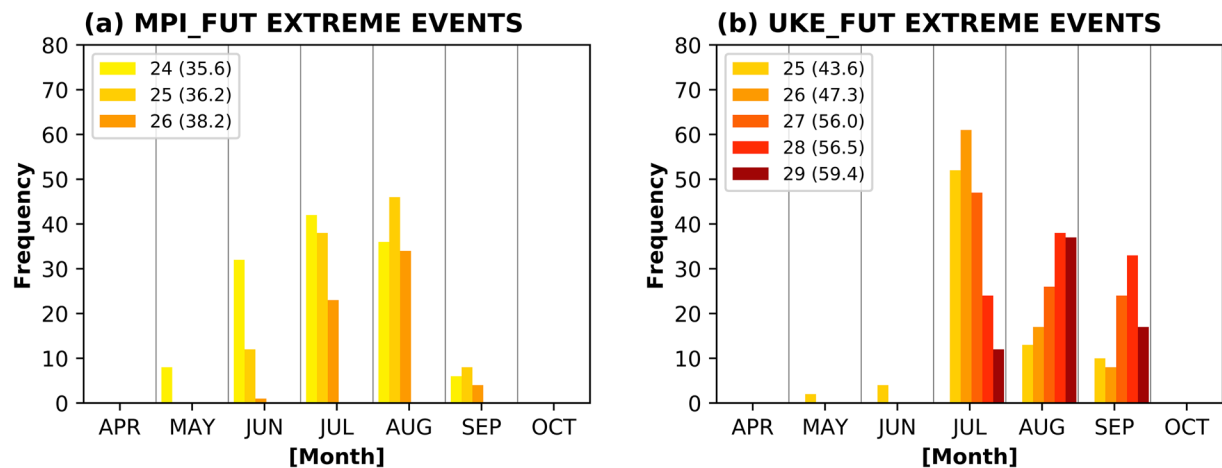


**Figure 4.** Future changes in extreme precipitation (EP) event frequency for each month (April to October) in future convection-permitting regional climate model simulations (CCLM2.5) forced by (a) MPI and (b) UKE boundary conditions. Only EP events for the extended dew point temperature ( $T_d$ ) ranges are considered ( $24^{\circ}\text{C}$ – $26^{\circ}\text{C}$  for MPI and  $25^{\circ}\text{C}$ – $29^{\circ}\text{C}$  for UKE, respectively). EP thresholds (mm/h) for each  $T_d$  are provided in parentheses.

projects little changes in convective fraction- $T_d$  relationships except for an increase of convective fraction in cold  $T_d$ s from 12 to  $15^{\circ}\text{C}$  (Figure 3f), which likely shapes future EP intensities in H-CAPE (Figure 3d). Results from L-CAPE cases display little change in CPRCM\_MPI and an overall weakening of non-convective EP in CPRCM\_UKE, not greatly affecting the total changes (dashed lines in Figures 3c and 3d).

The extension of temperature ranges into warmer levels implies warm season expansion (cf. Park et al., 2022), which would bring more frequent occurrences of EP events. In this respect, future changes in EP event frequency distribution are investigated for each month (April to October) focusing on the extended  $T_d$  ranges (Figure 4). Different colors represent  $T_d$  bins for the future extended  $T_d$  ranges and the numbers in parentheses indicate corresponding EP thresholds for CPRCM\_MPI and CPRCM\_UKE models, respectively (Figures 3a and 3b). Although  $T_d$  ranges are different between the two CPRCMs due to the different climate sensitivities of GCMs as discussed above, the projected change patterns in EP frequencies are consistent, showing overall increases across summer months. This demonstrates the increased occurrence of unprecedented hourly EP events in high emission scenarios. Both CPRCMs project that severe EP events (darker red colors in Figure 4) will increase more in late summer (August–September) than early summer (June–July). CPRCM\_UKE predicts more frequent extreme events than CPRCM\_MPI in accord with the greater extension of EP- $T_d$  scaling into warmer conditions (Figure 3). This shift of short-term heavy rain events into later summer is consistent with the delayed retreat of summer monsoon in East Asia (Ha et al., 2020; Kitoh et al., 2013). This projected change in EP seasonal timing provides an important implication for the impacts and adaptations in terms of the changing character of hydrological extreme events.

#### 4. Conclusions

This study analyzed the hourly extreme rainfall scaling with temperature over South Korea using CPRCM historical and future simulations. The role of convection is examined by dividing precipitation types associated with extreme rainfall events into convective and non-convective ones based on the CAPE. CPRCM simulations are forced by two GCM boundary conditions that have different warming rates. CPRCM simulations are found to capture the observed super C-C relation between EP and  $T_d$ . This EP- $T_d$  relation cannot be reproduced by RCMs that exhibit weaker CIN and thereby underestimate upward motion due to the use of convective parameterizations, confirming CPRCM's better skills at simulating short-term EP. The important role of convection in super C-C scaling is identified by comparing the scaling patterns from convective rainfall with those from non-convective type. As a fraction of convective extreme events increases rapidly with temperature, convective scaling is found to dominate the total scaling.

This dominance of convective precipitation in shaping the EP- $T_d$  relation holds in the late 21st century under high greenhouse gas emission scenarios. Under global warming,  $T_d$  ranges in South Korea are shifted into warmer

conditions where EP can occur, extending the EP scaling accordingly. When comparing two CPRCM simulations, changes in convective fraction with temperature are found to be important for shaping future patterns of the scaling. Further, it is revealed that the extended scaling into warmer temperatures results in increased occurrences of unprecedented hourly extreme rainfall events, more strongly during the late summer season. Future increase in short-term EP indicates the importance of global warming mitigation to avoid associated severe socioeconomic damages. The enhanced role of convection in the future is also found to be stronger when a GCM having a larger warming rate is used to drive CPRCM, indicating the importance of boundary conditions employed for CPRCM simulations.

Our results provide important implications for other regions. First, the role of convection in future changes in EP-T scaling remains uncertain even over Europe and North America. Particularly, different precipitation types have yet been considered, simply assuming that convective rainfall will dominate at higher temperatures. Purr et al. (2021) is the only study that compared the scaling between H-CAPE and L-CAPE events, and our results largely support their conclusions, suggesting that convection plays an enhanced role in future EP-T scaling across regions. Second, this is the first analysis of present and future short-term EP-T scaling using CPM simulations for the Asian monsoon region, including East Asia, demonstrating increases in hourly EP and associated risk of floods over the most populated region. In particular, projected increases in unprecedented hourly EP in late summer represents important changes in monsoon characteristics. Comparing two GCM boundary conditions also gives a useful insight into the physical mechanisms behind hydrological scaling.

It should be noted that large uncertainties can arise from inter-GCM differences as well as internal climate variability. Changes in East Asian monsoon precipitation are uncertain due to inter-GCM differences in dynamic effects, that is, monsoon circulation changes, more for mean precipitation (e.g., Endo et al., 2021; Ha et al., 2020). In contrast, extreme summer precipitation over East Asia is projected to increase with good inter-model agreement, being determined by thermodynamic effects, that is, moisture increases with warming (e.g., Lee et al., 2018). In this respect, we identify strong EP-Td relations and show that two GCMs with different climate sensitivities induce different extensions of EP intensities following corresponding warming levels. Further studies based on multiple GCMs are needed to assess the robustness of our findings and thereby better constrain future projections of the scaling over East Asia. As a way of reducing model uncertainties, some studies utilized the idealized Pseudo Global Warming (PGW) approach (e.g., Prein et al., 2017, 2021; Qing & Wang, 2021; Rasmussen et al., 2020), which drives a CPRCM using reanalysis later boundary conditions perturbed by multi-GCM averaged signal patterns. The PGW method is, however, limited in considering future changes in atmospheric circulations (Lucas-Picher et al., 2021). Reconciled approaches to overcome those limitations are required for better consideration of uncertainty factors (e.g., Dai et al., 2020; Lenderink et al., 2021; Trapp et al., 2021). It should also be noted that our results are based on a single CPRCM, which may have systematical biases. A recent multi-CPRCM study suggests more intense heavy precipitation in CCLM than the Weather Research and Forecasting (WRF) model over Europe and the Mediterranean region (Ban et al., 2021). Therefore, to quantify uncertainties in future projections of short-term EP and better identify the associated role of convection, multi-CPRCM simulations driven by multi-GCM boundary conditions are needed.

## Data Availability Statement

CCLM simulation data supporting the results are available from Mendeley Data at <https://doi.org/10.17632/syfmhntn2m2.1>. ERA5 hourly data are downloadable from Climate Data Store at <https://doi.org/10.24381/cds.adbb2d47> (single level) and <http://doi.org/10.24381/cds.bd0915c6> (pressure level).

## References

- Ahrens, B., & Leps, N. (2021). Sensitivity of convection permitting simulations to lateral boundary conditions in idealized experiments. *Journal of Advances in Modeling Earth Systems*, 13(12), e2021MS002519. <https://doi.org/10.1029/2021MS002519>
- Ban, N., Cailaud, C., Coppola, E., Pichelli, E., Sobolowski, S., Adinolfi, M., et al. (2021). The first multi-model ensemble of regional climate simulations at kilometer-scale resolution, part I: Evaluation of precipitation. *Climate Dynamics*, 57(1–2), 275–302. <https://doi.org/10.1007/s00382-021-05708-w>
- Ban, N., Schmidli, J., & Schär, C. (2014). Evaluation of the convection-resolving regional climate modeling approach in decade-long simulations. *Journal of Geophysical Research-Atmospheres*, 119(13), 7889–7907. <https://doi.org/10.1002/2014JD021478>
- Ban, N., Schmidli, J., & Schär, C. (2015). Heavy precipitation in a changing climate: Does short-term summer precipitation increase faster? *Geophysical Research Letters*, 42(4), 1165–1172. <https://doi.org/10.1002/2014GL062588>

## Acknowledgments

We thank two anonymous reviewers for their constructive comments. This study is supported by the Korea Meteorological Administration Research and Development Program under Grant KMI2020-01413 and the Human Resource Program for Sustainable Environment in the 4th Industrial Revolution Society. We acknowledge the members of the Climate Limited-area Modeling Community (CLM-Community) for their help in setting up the CCLM simulations. The CCLM simulations were performed by using the supercomputing resource of the Korea Meteorological Administration (National Center for Meteorological Supercomputer).



- Barbero, R., Fowler, H. J., Blenkinsop, S., Westra, S., Moron, V., Lewis, E., et al. (2019). A synthesis of hourly and daily precipitation extremes in different climatic regions. *Weather and Climate Extremes*, 26, 100219. <https://doi.org/10.1016/j.wace.2019.100219>
- Belusic, D., de Vries, H., Dobler, A., Landgren, O., Lind, P., Lindstedt, D., et al. (2020). HCLIM38: A flexible regional climate model applicable for different climate zones from coarse to convection-permitting scales. *Geoscientific Model Development*, 13(3), 1311–1333. <https://doi.org/10.5194/gmd-13-1311-2020>
- Berg, P., & Haerter, J. O. (2013). Unexpected increase in precipitation intensity with temperature—A result of mixing of precipitation types? *Atmospheric Research*, 119, 56–61. <https://doi.org/10.1016/j.atmosres.2011.05.012>
- Berg, P., Moseley, C., & Haerter, J. O. (2013). Strong increase in convective precipitation in response to higher temperatures. *Nature Geoscience*, 6(3), 181–185. <https://doi.org/10.1038/ngeo1731>
- Blenkinsop, S., Chan, S. C., Kendon, E. J., Roberts, N. M., & Fowler, H. J. (2015). Temperature influences on intense UK hourly precipitation and dependency on large-scale circulation. *Environmental Research Letters*, 10(5), 054021. <https://doi.org/10.1088/1748-9326/10/5/054021>
- Brisson, E., Van Weverberg, K., Demuzere, M., Devis, A., Saeed, S., Stengel, M., & van Lipzig, N. P. M. (2016). How well can a convection-permitting climate model reproduce decadal statistics of precipitation, temperature and cloud characteristics? *Climate Dynamics*, 47(9–10), 3043–3061. <https://doi.org/10.1007/s00382-016-3012-z>
- Busuioc, A., Baciu, M., Breza, T., Dumitrescu, A., Stoica, C., & Baghina, N. (2017). Changes in intensity of high temporal resolution precipitation extremes in Romania: Implications for Clausius-Clapeyron scaling. *Climate Research*, 72(3), 239–249. <https://doi.org/10.3354/cr01469>
- Chen, J., Dai, A., Zhang, Y., & Rasmussen, K. L. (2020). Changes in convective available potential energy and convective inhibition under global warming. *Journal of Climate*, 33(6), 2025–2050. <https://doi.org/10.1175/JCLI-D-19-0461.1>
- Dai, A., Rasmussen, R. M., Ikeda, K., & Liu, C. (2020). A new approach to construct representative future forcing data for dynamic downscaling. *Climate Dynamics*, 55(1–2), 315–323. <https://doi.org/10.1007/s00382-017-3708-8>
- Dobler, A., & Ahrens, B. (2010). Analysis of the Indian summer monsoon system in the regional climate model COSMO-CLM. *Journal of Geophysical Research*, 115(D16), D16101. <https://doi.org/10.1029/2009JD013497>
- Drobinski, P., Alonzon, B., Bastin, S., Da Silva, N., & Muller, C. (2016). Scaling of precipitation extremes with temperature in the French Mediterranean region: What explains the hook shape? *Journal of Geophysical Research-Atmospheres*, 121(7), 3100–3119. <https://doi.org/10.1002/2015JD023497>
- Endo, H., Kitoh, A., Mizuta, R., & Ose, T. (2021). Different future changes between early and late summer monsoon precipitation in East Asia. *Journal of the Meteorological Society of Japan Series II*, 99(6), 1501–1524. <https://doi.org/10.2151/jmsj.2021-073>
- Fosser, G., Kendon, E. J., Stephenson, D., & Tucker, S. (2020). Convection-permitting models offer promise of more certain extreme rainfall projections. *Geophysical Research Letters*, 47(13), e2020GL088151. <https://doi.org/10.1029/2020GL088151>
- Fosser, G., Khodayar, S., & Berg, P. (2015). Benefit of convection permitting climate model simulations in the representation of convective precipitation. *Climate Dynamics*, 44(1–2), 45–60. <https://doi.org/10.1007/s00382-014-2242-1>
- Fowler, H. J., Lenderink, G., Prein, A. F., Westra, S., Allan, R. P., Ban, N., et al. (2021). Anthropogenic intensification of short-duration rainfall extremes. *Nature Reviews Earth & Environment*, 2, 107–122. <https://doi.org/10.1038/s43017-020-00128-6>
- Fujibe, F. (2013). Clausius-Clapeyron-like relationship in multidecadal changes of extreme short-term precipitation and temperature in Japan. *Atmospheric Science Letters*, 14(3), 127–132. <https://doi.org/10.1002/asl2.428>
- Ha, K.-J., Moon, S., Timmermann, A., & Kim, D. (2020). Future changes of summer monsoon characteristics and evaporative demand over Asia in CMIP6 simulations. *Geophysical Research Letters*, 47(8), e2020GL087492. <https://doi.org/10.1029/2020GL087492>
- Hardwick Jones, R., Westra, S., & Sharma, A. (2010). Observed relationship between extreme sub-daily precipitation, surface temperature, and relative humidity. *Geophysical Research Letters*, 37(22), L22805. <https://doi.org/10.1029/2010GL045081>
- Hatsuzuka, D., Sato, T., & Higuchi, Y. (2021). Sharp rises in large-scale, long-duration precipitation extremes with higher temperatures over Japan. *Npj Climate and Atmospheric Science*, 4(1), 29. <https://doi.org/10.1038/s41612-021-00184-9>
- Helsen, S., van Lipzig, N. P. M., Demuzere, M., Vanden Broucke, S., Caluwaerts, S., De Cruz, L., et al. (2020). Consistent scale-dependency of future increases in hourly extreme precipitation in two convection-permitting climate models. *Climate Dynamics*, 54(3–4), 1267–1280. <https://doi.org/10.1007/s00382-019-05056-w>
- Hersbach, H., Bell, B., Berrisford, P., Hirahara, S., Horányi, A., Muñoz-Sabater, J., et al. (2020). The ERA5 global reanalysis. *Quarterly Journal of the Royal Meteorological Society*, 146(730), 1999–2049. <https://doi.org/10.1002/qj.3803>
- Huang, B., Polanski, S., & Cubasch, U. (2015). Assessment of precipitation climatology in an ensemble of CORDEX-East Asia regional climate simulations. *Climate Research*, 64(2), 141–158. <https://doi.org/10.3354/cr01302>
- Ivancic, T. J., & Shaw, S. B. (2016). A U.S.-based analysis of the ability of the Clausius-Clapeyron relationship to explain changes in extreme rainfall with changing temperature. *Journal of Geophysical Research-Atmospheres*, 121(7), 3066–3078. <https://doi.org/10.1002/2015JD024288>
- Juzbašić, A., Ahn, J.-B., Cha, D.-H., Chang, E.-C., & Min, S.-K. (2022). Changes in heat stress considering temperature, humidity, and wind over East Asia under RCP8.5 and SSP5-8.5 scenarios. *International Journal of Climatology*, 42(12), 6579–6595. <https://doi.org/10.1002/joc.7636>
- Kendon, E. J., Ban, N., Roberts, N., Fowler, H., Roberts, M., Chan, S., et al. (2017). Do convection-permitting regional climate models improve projections of future projection change? *Bulletin of the American Meteorological Society*, 98(1), 79–93. <https://doi.org/10.1175/BAMS-D-15-0004.1>
- Kendon, E. J., Stratton, R. A., Tucker, S., Marsham, J. H., Berthou, S., Rowell, D. P., & Senior, C. A. (2019). Enhanced future changes in wet and dry extremes over Africa at convection-permitting scale. *Nature Communications*, 10(1), 1794. <https://doi.org/10.1038/s41467-019-09776-9>
- Kitoh, A., Endo, H., Krishna Kumar, K., Cavalcanti, I. F. A., Goswami, P., & Zhou, T. (2013). Monsoons in a changing world: A regional perspective in a global context. *Journal of Geophysical Research-Atmospheres*, 118(8), 3053–3065. <https://doi.org/10.1002/jgrd.50258>
- Lee, D., Min, S.-K., Fischer, E., Shiogama, H., Bethke, I., Lierhammer, L., & Scinocca, J. F. (2018). Impacts of half a degree additional warming on the Asian summer monsoon rainfall characteristics. *Environmental Research Letters*, 13(4), 044033. <https://doi.org/10.1088/1748-9326/aab55d>
- Lenderink, G., Barbero, R., Loriaux, J. M., & Fowler, H. J. (2017). Super-Clausius-Clapeyron scaling of extreme hourly convective precipitation and its relation to large-scale atmospheric conditions. *Journal of Climate*, 30(15), 6037–6052. <https://doi.org/10.1175/JCLI-D-16-0808.1>
- Lenderink, G., de Vries, H., Fowler, H. J., Barbero, R., van Ulft, B., & van Meijgaard, E. (2021). Scaling and responses of extreme hourly precipitation in three climate experiments with a convection-permitting model. *Philosophical Transactions of the Royal Society A*, 379(2195), 20190544. <https://doi.org/10.1098/rsta.2019.0544>
- Lenderink, G., Mok, H. Y., Lee, T. C., & van Oldenborgh, G. J. (2011). Scaling and trends of hourly precipitation extremes in two different climate zones—Hong Kong and The Netherlands. *Hydrology and Earth System Sciences*, 15(9), 3033–3041. <https://doi.org/10.5194/hess-15-3033-2011>
- Lenderink, G., & van Meijgaard, E. (2010). Linking increases in hourly precipitation extremes to atmospheric temperature and moisture changes. *Environmental Research Letters*, 5(2), 025208. <https://doi.org/10.1088/1748-9326/5/2/025208>

- Lepore, C., Veneziano, D., & Molini, A. (2015). Temperature and CAPE dependence of rainfall extremes in the eastern United States. *Geophysical Research Letters*, 42(1), 74–83. <https://doi.org/10.1002/2014GL062247>
- Li, D., Von Storch, H., & Geyer, B. (2016). Testing reanalyses in constraining dynamical downscaling. *Journal of the Meteorological Society of Japan*, 94(0), 47–68. <https://doi.org/10.2151/jmsj.2015-044>
- Li, P., Furtado, K., Zhou, T., Chen, H., Li, J., Guo, Z., & Xiao, C. (2020). The diurnal cycle of East Asian summer monsoon precipitation simulated by the Met Office Unified Model at convection-permitting scales. *Climate Dynamics*, 55(1–2), 131–151. <https://doi.org/10.1007/s00382-018-4368-z>
- Loriaux, J. M., Lenderink, G., & Pier Siebesma, A. (2016). Peak precipitation intensity in relation to atmospheric conditions and large-scale forcing at midlatitudes. *Journal of Geophysical Research-Atmospheres*, 121(10), 5471–5487. <https://doi.org/10.1002/2015JD024274>
- Lucas-Picher, P., Argüeso, D., Brisson, E., Trambly, Y., Berg, P., Lemonsu, A., et al. (2021). Convection-permitting modeling with regional climate models: Latest developments and next steps. *Wiley Interdisciplinary Reviews: Climate Change*, 12(6), e731. <https://doi.org/10.1002/wcc.731>
- Maranan, M., Fink, A. H., Knippertz, P., Francis, S. D., Akpo, A. B., Jegede, G., & Yorke, C. (2019). Interactions between convection and moist vortex associated with an extreme rainfall event over southern West Africa. *Monthly Weather Review*, 147(7), 2309–2328. <https://doi.org/10.1175/MWR-D-18-0396.1>
- Meehl, G., Senior, A., Eyring, V., Flato, G., Lamarque, J.-F., Stouffer, R. J., et al. (2020). Context for interpreting equilibrium climate sensitivity and transient climate response from the CMIP6 Earth system models. *Science Advances*, 26, eaba1981. <https://doi.org/10.1126/sciadv.aba1981>
- Murata, A., Sasaki, H., Kawase, H., & Nosaka, M. (2017). Evaluation of precipitation over an oceanic region of Japan in convection-permitting regional climate model simulations. *Climate Dynamics*, 48(5–6), 1779–1792. <https://doi.org/10.1007/s00382-016-3172-x>
- Murata, A., Sasaki, H., Kawase, H., Nosaka, M., Aoyagi, T., Oh'izumi, M., et al. (2017). Projection of future climate change over Japan in ensemble simulations using a convection-permitting regional climate model with urban canopy. *Scientific Online Letters on the Atmosphere*, 13, 219–223. <https://doi.org/10.2151/sola.2017-040>
- Oh, S.-G., & Sushama, L. (2020). Short-duration extremes over Canada in a warmer climate. *Climate Dynamics*, 54(3–4), 2493–2509. <https://doi.org/10.1007/s00382-020-05126-4>
- O'Neill, B. C., Tebaldi, C., van Vuuren, D. P., Eyring, V., Friedlingstein, P., Hurtt, G., et al. (2016). The scenario model intercomparison project (ScenarioMIP) for CMIP6. *Geoscientific Model Development*, 9, 3461–3482. <https://doi.org/10.5194/gmd-9-3461-2016>
- Panthou, G., Mailhot, A., Laurence, E., & Talbot, G. (2014). Relationship between surface temperature and extreme rainfalls: A multi-time-scale and event-based analysis. *Journal of Hydrometeorology*, 15(5), 1999–2011. <https://doi.org/10.1175/JHM-D-14-0020.1>
- Park, B.-J., Min, S.-K., & Weller, E. (2022). Lengthening of summer season over the Northern Hemisphere under 1.5°C and 2.0°C global warming. *Environmental Research Letters*, 17(1), 014012. <https://doi.org/10.1088/1748-9326/ac3f64>
- Park, I.-H., & Min, S.-K. (2017). Role of convective precipitation in the relationship between subdaily extreme precipitation and temperature. *Journal of Climate*, 30(23), 9527–9537. <https://doi.org/10.1175/JCLI-D-17-0075.1>
- Pichelli, E., Coppola, E., Sobolowski, S., Ban, N., Giorgi, F., Stocchi, P., et al. (2021). The first multi-model ensemble of regional climate simulations at kilometer-scale resolution part 2: Historical and future simulations of precipitation. *Climate Dynamics*, 56(11–12), 3581–3602. <https://doi.org/10.1007/s00382-021-05657-4>
- Prein, A. F., Langhans, W., Fosser, G., Ferrone, A., Ban, N., Goergen, K., et al. (2015). A review on regional convection-permitting climate modeling: Demonstrations, prospects, and challenges. *Review of Geophysics*, 53(2), 323–361. <https://doi.org/10.1002/2014RG000475>
- Prein, A. F., Rasmussen, R. M., Ikeda, K., Liu, C., Clark, M. P., & Holland, G. J. (2017). The future intensification of hourly precipitation extremes. *Nature Climate Change*, 7(1), 48–52. <https://doi.org/10.1038/nclimate3168>
- Prein, A. F., Rasmussen, R. M., Wang, D., & Giangrande, S. E. (2021). Sensitivity of organized convective storms to model grid spacing in current and future climates. *Philosophical Transactions of the Royal Society A*, 379(2195), 20190546. <https://doi.org/10.1098/rsta.2019.0546>
- Purr, C., Brisson, E., & Ahrens, B. (2021). Convective rain cell characteristics and scaling in climate projections for Germany. *International Journal of Climatology*, 41(5), 3174–3185. <https://doi.org/10.1002/joc.7012>
- Qing, Y., & Wang, S. (2021). Multi-decadal convection-permitting climate projections for China's Greater Bay Area and surroundings. *Climate Dynamics*, 57(1–2), 415–434. <https://doi.org/10.1007/s00382-021-05716-w>
- Qiu, L., & Im, E.-S. (2021). Added value of high-resolution climate projections over South Korea on the scaling of precipitation with temperature. *Environmental Research Letters*, 16(12), 124034. <https://doi.org/10.1088/1748-9326/ac37d3>
- Raffa, M., Reeder, A., Adinolfi, M., & Mercogliano, P. (2021). A comparison between one-step and two-step nesting strategy in the dynamical downscaling of regional climate model COSMO-CLM at 2.2 km driven by ERA5 reanalysis. *Atmosphere*, 12(2), 260. <https://doi.org/10.3390/atmos12020260>
- Rasmussen, K. L., Prein, A. F., Rasmussen, R. M., Ikeda, K., & Liu, C. (2020). Changes in the convective population and thermodynamic environments in convection-permitting regional climate simulations over the United States. *Climate Dynamics*, 55(1–2), 383–408. <https://doi.org/10.1007/s00382-017-4000-7>
- Rio, C., Del Genio, A. D., & Hourdin, F. (2019). Ongoing breakthroughs in convective parameterization. *Current Climate Change Reports*, 5(2), 95–111. <https://doi.org/10.1007/s40641-019-00127-w>
- Rockel, B., Will, A., & Hense, A. (2008). The regional climate model COSMO-CLM (CCLM). *Meteorologische Zeitschrift*, 17(4), 347–348. <https://doi.org/10.1127/0941-2948/2008/0309>
- Roderick, T. P., Wasko, C., & Sharma, A. (2020). An improved covariate for projecting future rainfall extremes? *Water Resources Research*, 56(8), e2019WR026924. <https://doi.org/10.1029/2019WR026924>
- Sørland, S. L., Brogli, R., Kumar Pothapakula, P., Russo, E., Van de Walle, J., Ahrens, B., et al. (2021). COSMO-CLM regional climate simulations in the Coordinated Regional Climate Downscaling Experiment (CORDEX) framework: A review. *Geoscientific Model Development*, 14(8), 5125–5154. <https://doi.org/10.5194/gmd-14-5125-2021>
- Steger, C., & Bucchignani, E. (2020). Regional climate modelling with COSMO-CLM: History and perspectives. *Atmosphere*, 11, 1250. <https://doi.org/10.3390/atmos11111250>
- Sugimoto, S., & Takahashi, H. G. (2016). Effect of spatial resolution and cumulus parameterization on simulated precipitation over South Asia. *Scientific Online Letters on the Atmosphere*, 12(Special\_Edition), 7–12. <https://doi.org/10.2151/sola.12A-002>
- Suhas, E., & Zhang, G. J. (2015). Evaluating convective parameterization closures using cloud-resolving model simulation of tropical deep convection. *Journal of Geophysical Research-Atmospheres*, 120(4), 1260–1277. <https://doi.org/10.1002/2014JD022246>
- Trapp, R. J., Woods, M. J., Lasher-Trapp, S. G., & Grover, M. A. (2021). Alternative implementations of the “pseudo-global-warming” methodology for event-based simulations. *Journal of Geophysical Research: Atmospheres*, 126(24), e2021JD035017. <https://doi.org/10.1029/2021jd035017>
- Utsumi, N., Seto, S., Kanae, S., Maeda, E. E., & Oki, T. (2011). Does higher surface temperature intensify extreme precipitation? *Geophysical Research Letters*, 38(16), L16708. <https://doi.org/10.1029/2011GL048426>

- Visser, J. B., Wasko, C., Sharma, A., & Nathan, R. (2020). Resolving inconsistencies in extreme precipitation-temperature sensitivities. *Geophysical Research Letters*, *47*(18), e2020GL089723. <https://doi.org/10.1029/2020GL089723>
- Wang, D., Menz, C., Simon, T., Simmer, C., & Ohlwein, C. (2013). Regional dynamical downscaling with CCLM over East Asia. *Meteorology and Atmospheric Physics*, *121*(1–2), 39–53. <https://doi.org/10.1007/s00703-013-0250-z>
- Wang, H., Sun, F., & Liu, W. (2018). The dependence of daily and hourly precipitation extremes on temperature and atmospheric humidity over China. *Journal of Climate*, *31*(21), 8931–8944. <https://doi.org/10.1175/JCLI-D-18-0050.1>
- Wasko, C., & Sharma, A. (2014). Quantile regression for investigating scaling of extreme precipitation with temperature. *Water Resources Research*, *50*(4), 3608–3614. <https://doi.org/10.1002/2013WR015194>
- Wehner, M., Lee, J., Risser, M., Ullrich, P., Gleckler, P., & Collins, W. D. (2021). Evaluation of extreme sub-daily precipitation in high-resolution global climate model simulations. *Philosophical Transactions of the Royal Society A*, *379*(2195), 20190545. <https://doi.org/10.1098/rsta.2019.0545>
- Xiao, C., Wu, P., Zhang, L., & Song, L. (2016). Robust increase in extreme summer rainfall intensity during the past four decades observed in China. *Scientific Reports*, *6*(1), 38506. <https://doi.org/10.1038/srep38506>